

## Effect of Pd addition on porosity properties of $\gamma$ -Al<sub>2</sub>O<sub>3</sub> as a catalyst support material

Dwita Suastiyanti<sup>a,\*</sup>, Marlin Wijaya<sup>b</sup> and Byakta Gana Pandita<sup>c</sup>

<sup>a,c</sup>Department of Mechanical Engineering, Institut Teknologi Indonesia, Puspiptek Raya Street, Tangerang Selatan 15314 Indonesia

<sup>b</sup>Physics Research Centre, Badan Riset Inovasi Nasional, Puspiptek Raya Street, Tangerang Selatan, Indonesia 15314, Indonesia

The  $\gamma$ -Al<sub>2</sub>O<sub>3</sub> compound is generally not effective enough as catalyst, one of which is due to the low catalyst activity so that it is unable to break down the reactant into conventional fuel fractions. The sol gel process applied to form  $\gamma$ -Al<sub>2</sub>O<sub>3</sub> and Pd/ $\gamma$ -Al<sub>2</sub>O<sub>3</sub> powders at a calcination temperature of 350 °C for 2 hours and a sintering temperature of 450 °C for 4 hours produces homogeneous Pd/ $\gamma$ -Al<sub>2</sub>O<sub>3</sub> and  $\gamma$ -Al<sub>2</sub>O<sub>3</sub> powders and nanoparticles. These two materials can be used as catalyst support materials because they have adequate adsorption and desorption power where Pd/ $\gamma$ -Al<sub>2</sub>O<sub>3</sub> has a DA micropore volume (0.097 cc/g), pore volume (0.387 cc/g) and pore radius (46,868 Angstrom) which are greater than gamma. The Pd metal surface has the ability to bind substances will react to form reactive species. These metals accelerate gas reactions by forming weak bonds between gases and metal atoms on the surface. This process is called adsorption. The gases bound to metal surfaces react more easily than gases in the air. After the reaction occurs, the reaction products are released bond to the metal surface. This process is called desorption.

**Keywords:** Catalyst support, Adsorption, Desorption, Micropore, Sol-gel.

### Introduction

The  $\gamma$ -Al<sub>2</sub>O<sub>3</sub> compound is a transition alumina that is best known for its use as a catalyst support. Gamma alumina ( $\gamma$ -Al<sub>2</sub>O<sub>3</sub>) with a specific area of 160-300 m<sup>2</sup>/g plays a role as a support or catalyst support. Support is a component in a catalyst which functions to increase the surface area of the catalyst by providing a pore surface or as a template for the shape of the catalyst. Generally  $\gamma$ -Al<sub>2</sub>O<sub>3</sub> support is often used because the price is quite economical, has a stable structure, and its pore size can be varied. Support it is relatively stable at high temperatures, easy to shape, and has a point quite high melting, and suitable for reactions involving hydrogen because it requires a large surface area. The pore (crystal) size of the active components for industrial catalysts is at range 50-500 Å. Surface area decreases as size of crystal increases. Therefore, to obtain maximum activity, maximum surface area is needed, it is necessary to have as small of catalyst crystal as possible

In this research, the synthesis of the heterogeneous catalyst  $\gamma$ -Al<sub>2</sub>O<sub>3</sub> in nanoparticle size and single phase will be carried out using an easier and more economical method. Alumina is aluminum oxide and has properties as a heat insulator and electrical insulator that is good and resistant to high temperatures so it is often used as

a catalyst or solid catalyst support. Alumina has hard properties, is relatively stable at high temperature, large pore structure, easy to shape, and has high melting point. These characteristics cause alumina to be widely used as an adsorbent, catalyst, sandpaper, and in other chemical industrial fields. The  $\gamma$ -Al<sub>2</sub>O<sub>3</sub> nanoparticle compound as a Pt-Pd catalyst support is the most popular type of material because it has a large area and is relatively stable at temperature intervals in most catalytic reactions. The  $\gamma$ -Al<sub>2</sub>O<sub>3</sub> compound is generally not effective enough, one of which is due to the low catalyst activity so that it is unable to break down the reactant into conventional fuel fractions. In addition, catalyst activity is limited by the formation of coke and the catalyst pores are closed by coke [1]. The Pd metal surface has the ability to bind substances will react to form reactive species. these metals accelerate gas reactions by forming weak bonds between gases and metal atoms on the surface. This process is called adsorption. The gases bound to metal surfaces react more easily than gases it is in the air. After the reaction occurs, the reaction products are released bond to the metal surface. This process is called desorption. Palladium-based catalysts are reported to have good capabilities in hydrogenation and hydrodeoxygenation reactions. The use of Pd supported by active carbon is able to hydrogenate pentene into pentane with a conversion of 99.8% and the product produced is 98.6%.

One way to improve the performance of a catalyst is to make it nanoparticle in size. The use of nanoparticle

\*Corresponding author:  
Tel: +62-85697163727  
Fax: +62-7561091  
E-mail: [dwita\\_suastiyanti@iti.ac.id](mailto:dwita_suastiyanti@iti.ac.id)

catalysts using the ZSM-5 catalyst in cracking LDPE (Low Density Polyethylene). The results obtained show that ZSM-5 nanoparticles have higher catalytic activity than microparticle [2]. La-doped BaTiO<sub>3</sub> (BLaxT) ceramics, with  $x = (0, 0.25, 0.50, 0.75, 1.5 \text{ and } 3\%)$  were prepared using the sol gel method; the choice of this method of processing was based on its various advantages, low processing temperature, high purity, homogeneity and an excellent control of the stoichiometry of the products [3]. It has investigated the structural properties of the samples using X-ray diffraction (XRD), Fourier Transform Infrared (FT-IR) spectroscopy, Raman spectroscopy and scanning electron microscopy (SEM) [4]. We have also performed dielectric measurements for temperatures such as  $50 < T < 300 \text{ }^\circ\text{C}$ . Experimental results were analysed and then discussed as functions of the doping concentration, and compared to those reported in the literature [5].

Therefore, in this research, the size of the  $\gamma\text{-Al}_2\text{O}_3$  compound will be made in nanoparticle size. One way to improve the performance of a catalyst is to make it nanoparticle in size. In addition, the porosity of Al<sub>2</sub>O<sub>3</sub> greatly influences the ability of the catalyst to absorb gas.

The method used in this research is the sol gel method because this method has many advantages, including the process taking place at low temperatures, the process is relatively easier, can be applied in all conditions (versatile), produces products with high purity and homogeneity if the parameters are varied. Apart from that, what is most impressive about the sol-gel process is that the cost is relatively cheap and the product in the form of silica xerogel produced is not toxic [6]. In research conducted by Dwita Suastiyanti et al. 2021, the modified weight ratio of BaTiO<sub>3</sub>:BiFeO<sub>3</sub> were 2:1 has the potential to produce ceramic powder with particle size 72-81 nm (sintered at 700 °C for 6 hours) [7, 8]. Meanwhile, the  $\gamma\text{-Al}_2\text{O}_3$  compound which

is widely available on the market as a commercial product is obtained at an expensive price and is not yet in nanoparticle and single phase form. With the sol gel method, it is hoped to produce  $\gamma\text{-Al}_2\text{O}_3$  and Pd/ $\gamma\text{-Al}_2\text{O}_3$  compounds in the form of nanoparticles, single phase and have a large volume, surface area and pore radius.

The novelty of this research lies in the material structure, namely powder in a bulk and single phase system as well as in the form of nanoparticles using simple and easy technology with the future target being that it can be applied in industry. The bulk system must be on a nanometer phase size scale, having large surface area so that extensive interaction can occur between Pd ions and  $\gamma\text{-Al}_2\text{O}_3$  cavities in a material system. With the nanometer scale  $\gamma\text{-Al}_2\text{O}_3$  particle size, it is expected to produce powder with a surface area that can significantly increase interaction. Therefore, it is hoped that the benefits from this research activity can be taken, namely the production of new methods, namely sol-gel with certain conditions for the synthesis of single-phase Pd/ $\gamma\text{-Al}_2\text{O}_3$  buffer materials and nanoparticles.

The surface area of alumina depends on the degree of aggregation and discontinuity of the alumina gel grains during the aging process, which is strongly influenced by the pH of precipitation. In this connection, it is observed that at acidic pH (pH = 6), aggregation of alumina gel granules may form, leading to the formation of oxides

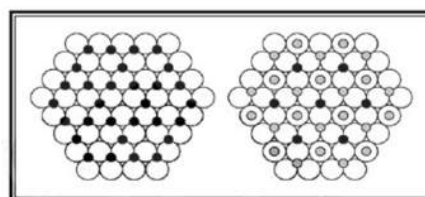


Fig. 1. The First Two Layers of the  $\gamma\text{-Al}_2\text{O}_3$  Structure.

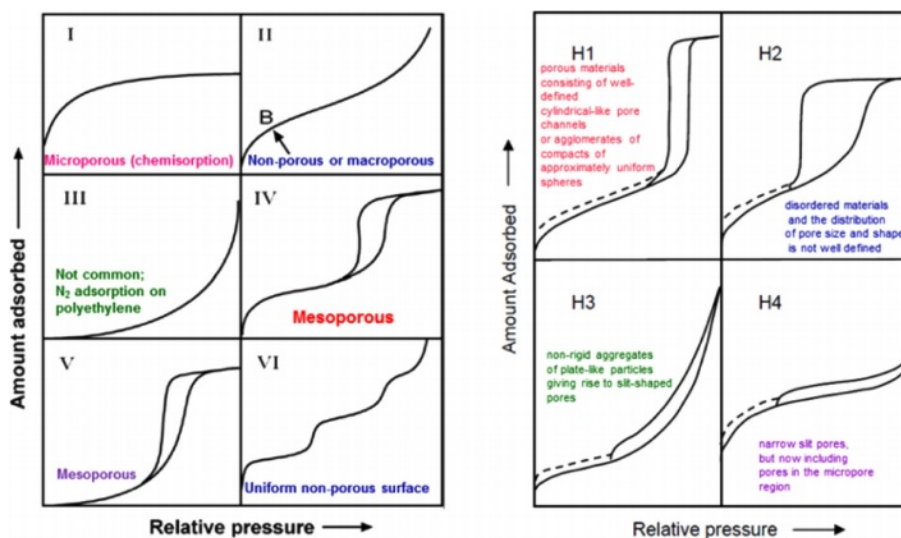


Fig. 2. Relative Pressure vs Amount Adsorbed of Mesoporous.

with smaller pores and high surface area, while at higher pH (pH = 7-8) alumina gel granules break down which results in the formation of oxide with larger pores and a smaller surface area. Gamma Al<sub>2</sub>O<sub>3</sub> ( $\gamma$ -Al<sub>2</sub>O<sub>3</sub>) is a transition alumina and is an amorphous solid that has a deformed spinel structure, where the oxygen ions form dense cubic packing (ccp), which has 16 octahedral holes and 8 tetrahedral holes. Al<sup>3+</sup> ions occupy octahedral and tetrahedral coordination in the oxygen lattice. The octahedral Al<sup>3+</sup> structure is surrounded by 6 atom of O<sup>2-</sup> and the tetrahedral Al<sup>3+</sup> structure is surrounded by 4 atom of O<sup>2-</sup> as shown in Fig. 1.

The presence of a hysteresis curve (Fig. 2) shows that the mesoporous type IV (diameter of 2-50 nm) has a non-uniform distribution of size and shape (type H2). Step uptake at small P/Po (initial curve) shows adsorbent (solid interface)-adsorptive (N<sub>2</sub> adsorbed) interactions in the molecular dimension when filling shows micropores due to the sharp slope of the initial uptake curve. The widening of the hysteresis curve shows the binding of N<sub>2</sub> on the surface (capillary condensation-evaporation) and the presence of a slope (accompanied by a stepwise Al<sub>2</sub>O<sub>3</sub>) shows multilayer adsorption [9, 10].

## Experimental

The experimental method chosen is the sol-gel method. The flow diagram of research activities can be shown in Fig. 3.

The basic material used is Al(NO<sub>3</sub>)<sub>3</sub>·9H<sub>2</sub>O, citric acid (C<sub>6</sub>H<sub>8</sub>O<sub>7</sub>) Ammonium hydroxide (NH<sub>4</sub>OH), Pd(NO<sub>3</sub>)<sub>2</sub>, Aquabdestilate (H<sub>2</sub>O<sub>2</sub>). These basic materials are used to produce  $\gamma$ -Al<sub>2</sub>O<sub>3</sub> and Pd/ $\gamma$ -Al<sub>2</sub>O<sub>3</sub> powder. To produce Pd/ $\gamma$ -Al<sub>2</sub>O<sub>3</sub>, it has been added Pd(NO<sub>3</sub>)<sub>2</sub>. Synthesis is carried out using the sol-gel method where all the basic ingredients are heated on a hot plate at a temperature of 70-80 °C until a gel forms. Then the gel was dried at a temperature of 90 °C for 3 hours. After that, the

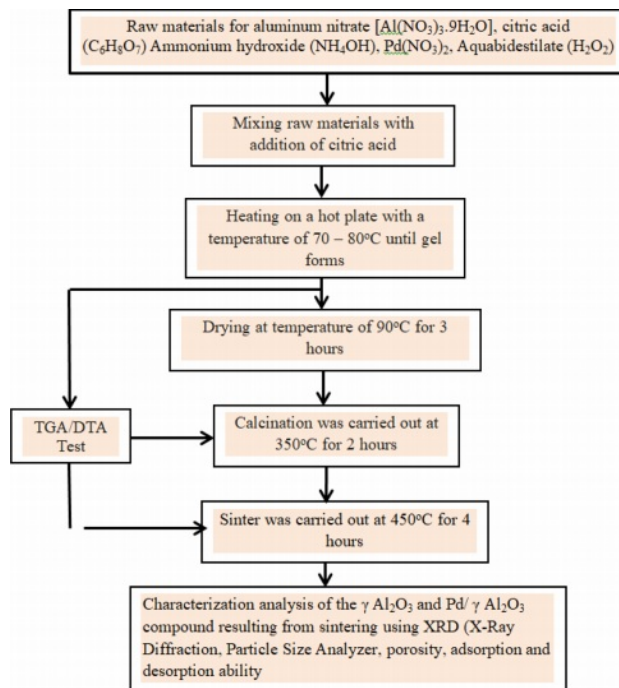


Fig. 3. Flowchart of Research Activity.

calcination process was carried out at temperatures of 350 °C for 2 hours. Finally, the sintering process was carried out at a temperature of 450 °C for 4 hours. The characteristics carried out on  $\gamma$ -Al<sub>2</sub>O<sub>3</sub> and Pb/ $\gamma$ -Al<sub>2</sub>O<sub>3</sub> powders are X-Ray Diffraction testing (to confirm the phase formed), Particle Size Analyzer (to determine particle size), Porosity and adsorption and desorption capabilities.

## Results and Discussion

### X-Ray Diffraction Test (XRD Test)

The XRD test results for  $\gamma$ -Al<sub>2</sub>O<sub>3</sub> powder are shown

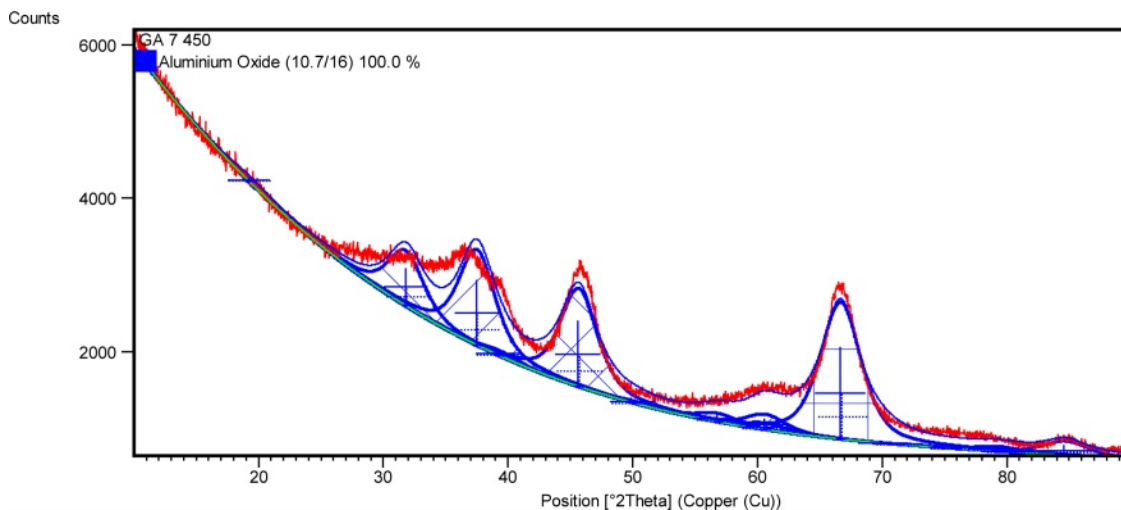


Fig. 4. X-Ray Diffraction Pattern of  $\gamma$ -Al<sub>2</sub>O<sub>3</sub>.

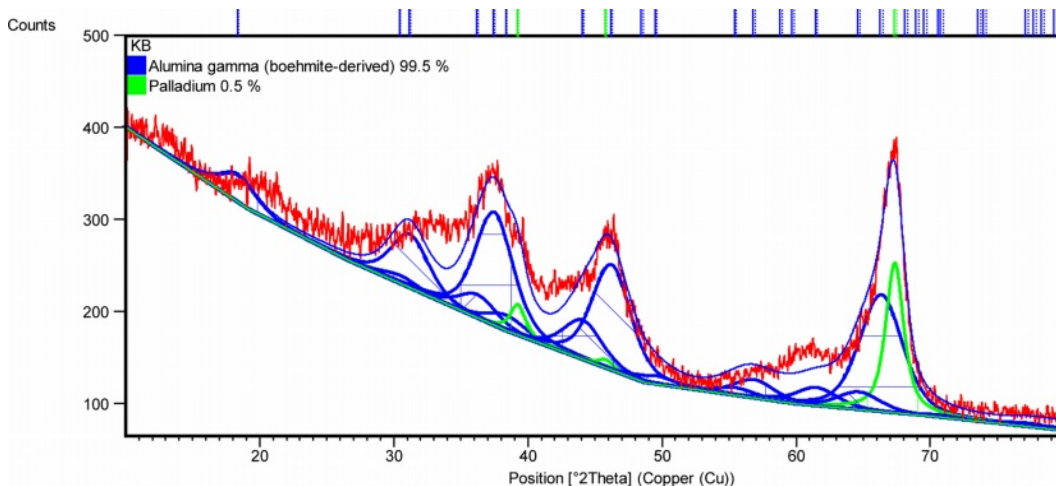


Fig. 5. X-Ray Diffraction Pattern of Pd/  $\gamma$ -Al<sub>2</sub>O<sub>3</sub>.

in Fig. 4. Based on observations in Fig. 4, it can be seen that the synthesis process using sol-gel produces 100% of the  $\gamma$ -Al<sub>2</sub>O<sub>3</sub> phase (single phase) and is in crystal form.

Meanwhile, the XRD test results for Pd/ $\gamma$ -Al<sub>2</sub>O<sub>3</sub> are shown in Fig. 5. Based on observations in Fig. 5, it can be seen that the sintering process using the sol-gel method produces a powder consisting of 99.5%  $\gamma$ -Al<sub>2</sub>O<sub>3</sub> and 0.5% Pd according to the initial composition during synthesis.

Fig. 4 and 5 prove that the synthesis process using a calcination temperature of 350 °C for 2 hours and a sintering temperature of 450 °C for 4 hours are the right parameters to produce  $\gamma$ -Al<sub>2</sub>O<sub>3</sub> and Pd/ $\gamma$ -Al<sub>2</sub>O<sub>3</sub> powders according to the expected composition. These process parameters also produce nanometer-sized powder as

Table 1. Particle Size of Pd/ $\gamma$ -Al<sub>2</sub>O<sub>3</sub> dan  $\gamma$ -Al<sub>2</sub>O<sub>3</sub>.

Powder	Size 1 (nm)	Size 2 (nm)	Size 3 (nm)	Average (nm)
$\gamma$ -Al <sub>2</sub> O <sub>3</sub>	73	72	75	73
Pd/ $\gamma$ -Al <sub>2</sub> O <sub>3</sub>	82	79	80	80

shown in Table 1.

Pd/ $\gamma$ -Al<sub>2</sub>O<sub>3</sub> powder has a larger particle size because the Pd<sup>2+</sup> ion has an average ionic radius of 0.75 Angstrom, which is larger than the Al<sup>3+</sup> ionic radius of 0.47 Angstrom. Powder particles that have a finer size have a larger surface area so they have a greater adsorption capacity. This is linear with the results of

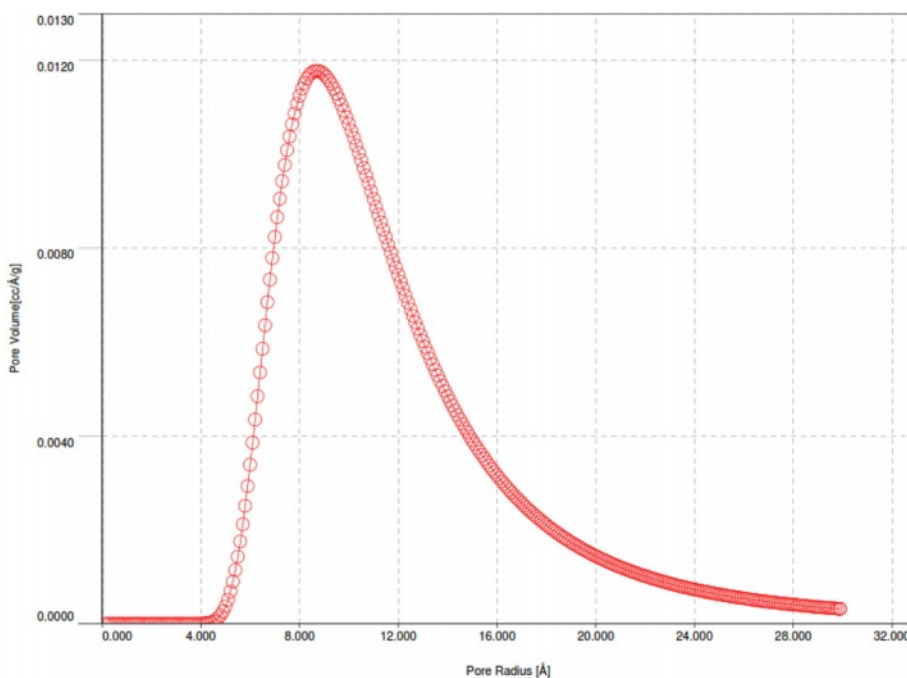


Fig. 6. Curve of Desorption Adsorption (DA) Analysis of Pd/ $\gamma$ -Al<sub>2</sub>O<sub>3</sub>.

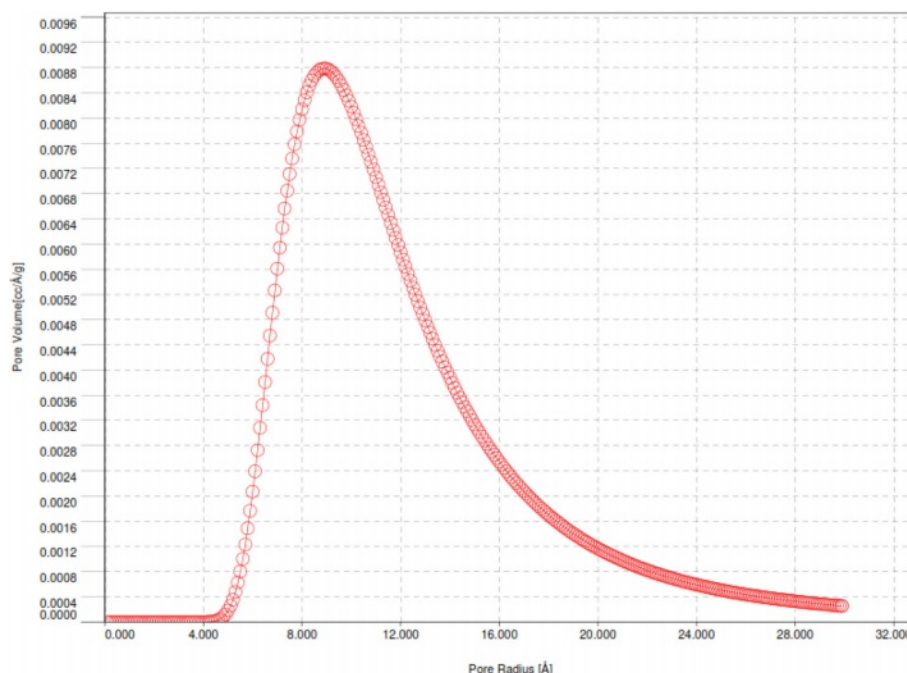


Fig. 7. Curve of Desorption Adsorption (DA) Analysis of  $\gamma$ -Al<sub>2</sub>O<sub>3</sub>.

desorption adsorption (DA) analysis and the results of observations of pore volume and radius as shown in Fig. 6, 7, 8 and 9

The curves in Fig. 7 and 8 show the same shape, only for Pd/ $\gamma$ -Al<sub>2</sub>O<sub>3</sub> the peak of the curve shifts to the right and higher which indicates a larger Pd/ $\gamma$ -Al<sub>2</sub>O<sub>3</sub> micropore volume. This shows that the adsorption and desorption capabilities of Pd/ $\gamma$ -Al<sub>2</sub>O<sub>3</sub> are better than  $\gamma$ -Al<sub>2</sub>O<sub>3</sub> so that the ability of Pd/ $\gamma$ -Al<sub>2</sub>O<sub>3</sub> as a catalyst support material for chemical processes is better than  $\gamma$

Table 2. Pore Radius and V Micropore Volume of Pd/ $\gamma$ -Al<sub>2</sub>O<sub>3</sub> and  $\gamma$ -Al<sub>2</sub>O<sub>3</sub>.

	DA Micropore Volume (cc/g)	Pore Radius (Angstrom)
Pd/ $\gamma$ -Al <sub>2</sub> O <sub>3</sub>	0.097	8.700e+00A
$\gamma$ -Al <sub>2</sub> O <sub>3</sub>	0.074	8.900e+00A

Al<sub>2</sub>O<sub>3</sub>. The characteristics in Fig. 6 and 7 can also be outlined in Table 2. The pore (crystal) size of the active

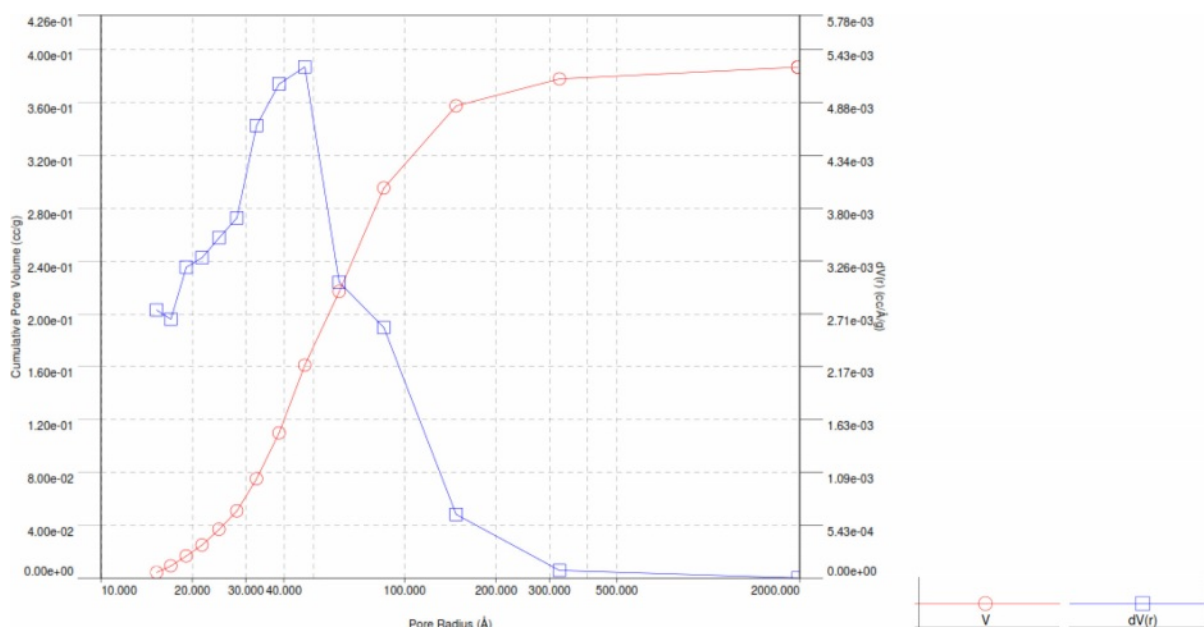


Fig. 8. Curve of BJH Adsorption of Pd/ $\gamma$ -Al<sub>2</sub>O<sub>3</sub>.

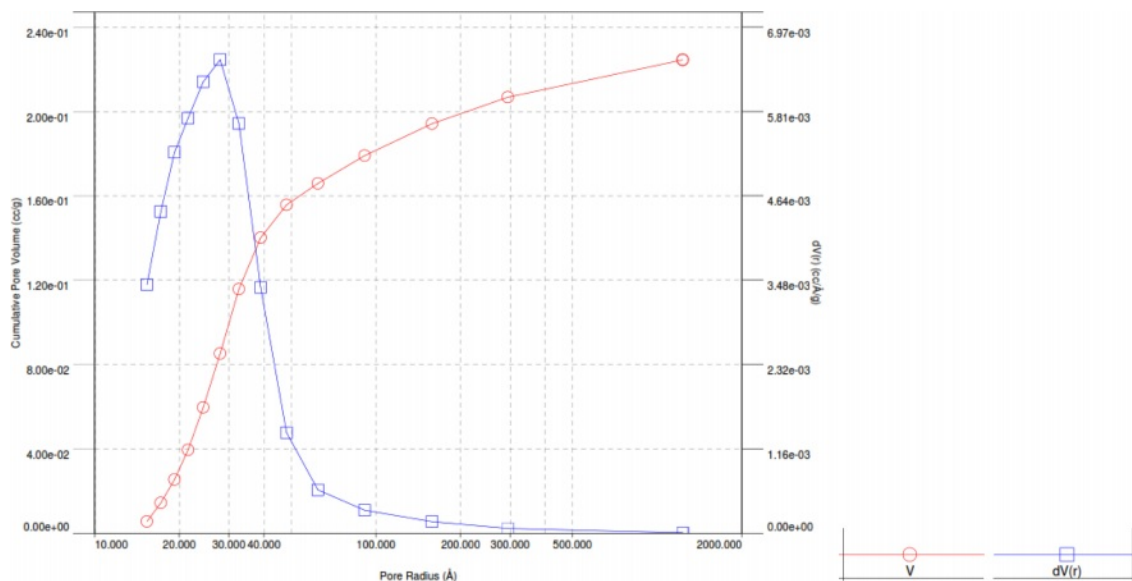


Fig. 9. Curve of BJH Adsorption of  $\gamma$ -Al<sub>2</sub>O<sub>3</sub>.

components for industrial catalysts is at range 50-500 Å. Surface area decreases as size increases crystal. So to get maximum activity you need space maximum surface area, it is necessary to have as small a catalyst crystal as possible.

Pore radius and pore volume analysis based on the Barrett-Joyner-Halenda (BJH) method for Pd/ $\gamma$ -Al<sub>2</sub>O<sub>3</sub> and  $\gamma$ -Al<sub>2</sub>O<sub>3</sub> powders is displayed with the BJH adsorption curve as shown in Fig. 8 and 9.

Based on Fig. 8 and 9, the pore radius and volume of Pd/ $\gamma$ -Al<sub>2</sub>O<sub>3</sub> are greater than  $\gamma$ -Al<sub>2</sub>O<sub>3</sub>. This also shows that the adsorption and desorption capabilities of Pd/ $\gamma$ -Al<sub>2</sub>O<sub>3</sub> are better than  $\gamma$ -Al<sub>2</sub>O<sub>3</sub>. The Pd metal surface has the ability to bind substances will react to form reactive species. These metals accelerate gas reactions by forming weak bonds between gases and metal atoms on

Table 3. Characteristic Based on BJH Adsorption.

	Pore Volume (cc/g)	Pore Radius (Å)
Pd/ $\gamma$ -Al <sub>2</sub> O <sub>3</sub>	0.387	46.868
$\gamma$ -Al <sub>2</sub> O <sub>3</sub>	0.224	27.936

the surface. This process is called adsorption. The gases bound to metal surfaces react more easily than gases in the air. After the reaction occurs, the reaction products are released bond to the metal surface. This process is called desorption [11-19]. The characteristics in Fig. 9 and 10 can also be outlined in Table 3.

The adsorption and desorption curves of Pd/ $\gamma$ -Al<sub>2</sub>O<sub>3</sub> and  $\gamma$ -Al<sub>2</sub>O<sub>3</sub> are shown in Fig. 10.

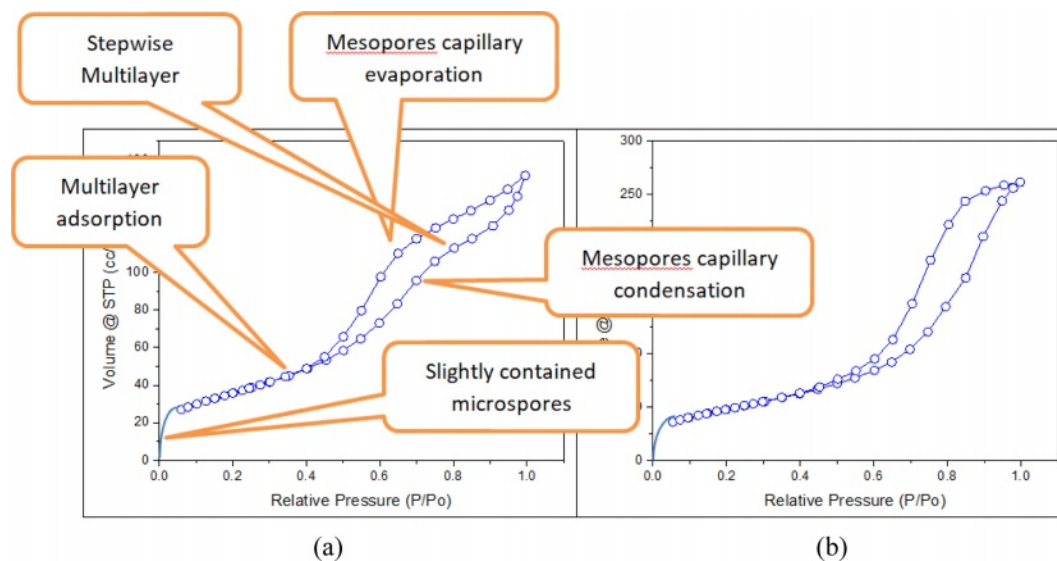


Fig. 10. Curve of Adsorption and Desorption of  $\gamma$ -Al<sub>2</sub>O<sub>3</sub> (a) and Pd/ $\gamma$ -Al<sub>2</sub>O<sub>3</sub> (b).

Fig. 10 shows the adsorption and desorption stages starting from the formation of a few micro pores then capillary condensation of micro pores occurs, followed by gradual multilayer formation then capillary evaporation of mesopores occurs and finally multilayer adsorption occurs [20-33].

### Conclusions

From the results of this research it could be concluded that the DA micropore volume, pore volume and pore radius of Pd/ $\gamma$ -Al<sub>2</sub>O<sub>3</sub> are greater than  $\gamma$ -Al<sub>2</sub>O<sub>3</sub>. This makes Pd/ $\gamma$ -Al<sub>2</sub>O<sub>3</sub> more suitable for use as a support material for chemical process catalysts. This is also supported by the smaller Pd/ $\gamma$ -Al<sub>2</sub>O<sub>3</sub> particle size compared to the  $\gamma$  Al<sub>2</sub>O<sub>3</sub> particle size. The sol gel process parameters used for the synthesis of Pd/ $\gamma$ -Al<sub>2</sub>O<sub>3</sub> and  $\gamma$ -Al<sub>2</sub>O<sub>3</sub> (calcination at 350 °C for 2 hours and sintering at 450 °C for 4 hours) produced a homogenous phase for both powders.

### References

- X. Li, J. Ceram. Process. Res. 23[1] (2022) 53-56.
- D. Suastiyanti, M.T.E. Manawan, and S. Handayani, The Int Journal of Eng. and Sc. 5[5] (2016) 118-124.
- A. Moutaouaffiq, M. Belhajji, A. Rjeb, and S. Sayouri, J. Ceram. Process. Res. 23[5] (2022) 570-582.
- B.M. Cunha, V.T.S. Aragao, C.O.D. Martins, and R.M. P.B. Oliveira, J. Ceram. Process. Res. 20[2] (2019) 133-138.
- S.D. Yudianto, S.A. Chandra, R. Roberto, D.P. Utama, V.O. Herlina, and Lusiana, J. Ceram. Process. Res. 23[3] (2022) 287-291.
- M.F. Zawrah, A.A. El-Kheshen, and H. Abd-El-All, J. of Ovonic Res. 5[5] (2009) 129-133.
- D. Suastiyanti and Y.N. Maulida, J. Ceram. Process. Res. 22[1] (2021) 61-65.
- D. Suastiyanti, Y.N. Maulida, and M. Wijaya, Key Eng. Mater. 867 (2020) 54-61.
- J. Kwon, K.H. Kim, H.J. Ahn, and Y. Hwang, J. Ceram. Process. Res. 22[2] (2021) 186-191.
- S. Yu, J. Ceram. Process. Res. 24[3] (2023) 503-506.
- K.N. Fatema, H.M. Lim, J.S. Hong, K.S. Lee, and L.J. Kim, J. Ceram. Process. Res. 24[1] (2023) 197-204.
- A.B. Prasetyo, M. Handayani, E. Sulistiyono, F. Firdiyono, E. Febriana, W. Mayangsari, S. Wahyuningsih, E. Pramono, A. Maksum, R. Riastuti, and J.W. Soedarsono, J. Ceram. Process. Res. 24[1] (2023) 103-110.
- S. Chen, J. Ceram. Process. Res. 23[1] (2022) 48-52.
- D. Lee, H.S. Hong, H. Jeong, and S.S. Ryu, J. Ceram. Process. Res. 23[2] (2022) 149-153.
- N.T.M. Nguyet, N.H.H. Phuc, V.D. Vuong, C.T.V. Khai, C.M.T. Phong, and L.V. Thang, J. Ceram. Process. Res. 20[2] (2019) 148-151.
- J.S. Park, J.G. Yeo, S.C. Yang, and C.H. Cho, J. Ceram. Process. Res. 19[1] (2018) 20-24.
- A. Maddu, I. Deni, and I. Sofian, J. Ceram. Process. Res. 19[1] (2018) 25-31.
- A.E. Ghandouri, S. Sayouri, T.E. Lamcharfi, and L. Hajji, J. Ceram. Process. Res. 19[2] (2018) 154-170.
- O.M. Serrato and J.S. Rodriguez, J. Ceram. Process. Res. 19[4] (2018) 306-310.
- W.Y. Jang, B. Basnet, J.G. Park, H.M. Lim, T.Y. Lim, and I.J. Kim, J. Ceram. Process. Res. 19[4] (2018) 296-301.
- Y.N. Lee, S.H.A.H. Nam, and K.W. Nam, J. Ceram. Process. Res. 19[6] (2018) 467-471.
- J. He, X. Zhang, J. Lian, and X. Zhang, J. Ceram. Process. Res. 25[1] (2024) 144-150.
- N. Rajasekaran, C. Muniraj, T. Venskatesan, and A. Kumaravel, J. Ceram. Process. Res. 25[1] (2024) 104-118.
- Z. Li, J. Ceram. Process. Res. 25[1] (2024) 92-96.
- J.S. Kim, U.S. Kim, J.H. Choi, J.H. Kim, and K.S. Han, J. Ceram. Process. Res. 25[1] (2024) 65-71.
- Z. Chen, S. Zhu, Q. Wang, and X. Wang, J. Ceram. Process. Res. 25[1] (2024) 56-64.
- B.J. Park, J.E. Lim, J.S. Yuk, S.H. Lee, M.G. Lee, J.S. Park, and S.G. Lee, J. Ceram. Process. Res. 25[1] (2024) 48-55.
- L. Gao, Y. Zhang, X. Yang, Y. He, and L. Song, J. Ceram. Process. Res. 21[6] (2020) 615-621.
- M.S. Kwon, J.W. Kim, J.S. Park, and S.G. Lee, J. Ceram. Process. Res. 21[6] (2020) 725-730.
- S. Li, M. Ma, Y. Tian, R. Li, X. Hu, and P. Liu, J. Ceram. Process. Res. 24[4] (2023) 693-699.
- Y. Liu, K. Luan, J. Xu, Z. Wang, Y. He, and G. Liu, J. Ceram. Process. Res. 24[4] (2023) 723-727.
- T. Nithyanandhan and R. Ramamoorthi, J. Ceram. Process. Res. 22[4] (2021) 369-376.
- N. Canikoglu, J. Ceram. Process. Res. 22[3] (2021) 258-263.